ICSO 2016

International Conference on Space Optics

Biarritz, France

18–21 October 2016

Edited by Bruno Cugny, Nikos Karafolas and Zoran Sodnik

HgCdTe detectors for space and science imaging in France: general issues and latest achievements

O. Gravrand

J. Rothman

C. Cervera

N. Baier

et al.

HGCDTE DETECTORS FOR SPACE AND SCIENCE IMAGING IN FRANCE: GENERAL ISSUES AND LATEST ACHIEVEMENTS

O. Gravrand[1], J. Rothman[1], C. Cervera[1], N. Baier[1], C. Lobre[1], J.P. Zanatta[1]
O. Boulade[2], V. Moreau[2], B. Fieque[3]
[1]CEA-LETI, France, [2]CEA-IRFU, France, [3]Sofradir, France

I. INTRODUCTION

HgCdTe is very unique material system for infrared (IR) detection. In combination with its lattice matched native substrate CdZnTe, this semiconductor alloy allows to address the whole infrared (IR) band, from the near IR (NIR, 2µm cutoff) to the middle wave IR (MWIR, 5µm cutoff), the long wave IR (LWIR, 10µm cutoff), up to the very long wave IR (VLWIR, cutoffs larger than 14µm). The versatility of this material lies in the fact that its bandgap might be modified with no significant change in its lattice parameter. Therefore, complex heterostructures might be used to optimize the performance of photodiodes built with this material. In this context, the use of molecular beam epitaxy (MBE) instead of the classical liquid phase epitaxy (LPE) might be very useful in the optimization of such high performance photodiodes. However, LPE grown based structures might still be considered for ultra-high performances. Indeed, LPE facilitates the Cd composition control, particularly for the narrow bandgaps corresponding to LWIR and VLWIR detection bands, especially when dealing with large production series. Moreover, the production yield of very high crystalline quality layers remains in favor of LPE in most of the wavebands of interest considered in this paper. This paper will first introduce the general issues concerning space and science imaging, both in terms of quantum efficiency (QE) and noise (i.e. dark current). This communication will then review our latest achievements in terms of IR focal plane for science in the NIR range for astronomy needs, but also MWIR and LWIR range for exoplanet search. At last, the discussion will focus on VLWIR arrays for atmospheric sounding.

II. SPACE AND SCIENCE IMAGING GENERAL ISSUES

What makes space and science applications so different from tactical systems? First of all, space and science imaging are very demanding in terms of high performance photodetection. Moreover, the need for pixel pitches is slightly different from tactical systems. Actually, space applications can be separated into two main categories. First, the focal plane array might stare at the Earth for weather forecasting, Earth monitoring or defense purposes. In this case, the photons involved in the detection might come from two different sources: the sun light reflected on the observed surface (in visible and NIR) or the IR emission of the earth itself as a black body at longer wavelengths. As a consequence, for wide band imaging, the detection might rely on a relatively large number of photons depending on the spectral band and the optics F number of the system. However, when the detected spectral band is narrow (in the case of hyperspectral detection for instance), the number of detected photons might drop drastically leading to low flux scenarii. In those two latter cases, the main issue remains the operating temperature where the detection specifications are met. Indeed, the power budget is a very important parameter in space applications, and the power of the detection block is highly dominated by the cooling temperature required. Another issue might also be the array format because the pixel pitch directly translates into image spatial resolution or alternatively spectral resolution in the case of diffractive spectroscopy, as will be further discussed later in this paper for astronomy applications.

Alternatively the focal plane array may stare at the outer space. In the case of astronomy observations, the cosmological redshift implies the fact that the information carried out by visible photons for close stars is shifted to the near IR range for far away objects. Hence, the spectral band of interest is mostly dominated by Visible and NIR for conventional astronomy observations. In most of the outer space observations, the incoming photons are emitted from far away objects and the number of detected photons is usually very low. Therefore, this kind of application deals with low to very low fluxes. Consequently the detection performance matters above all. The QE must be very high in order not to lose any of those precious photons. Moreover, the information carried out by those few photons must not be degraded by any additional noise, neither from the ROIC nor from the photodiode itself. As a consequence, the dark current has to be very low, typically below fractions of electrons per seconds. Besides, the observation of exoplanets is also a growing demand and usually requires longer wavelengths, MWIR to LWIR. The driving idea is the search of habitable exoplanets, which corresponds to a strong societal request. Different concepts are studied but one of the most demanding system is transit spectroscopy. The idea is to observe a slight change in the star emitted spectrum due to its planet absorption (absorption in its atmosphere or in the planet itself in the case of gas planets). This spectral change during planet transit might carry some information on the nature of the gas. In that case, the required spectral bands highly depend on the science goals. In other

words, it depends on the different components investigated in the observed exoplanet (water, carbon dioxide, methane or other molecules…). This detection concept is very demanding on detector performances. The incoming photon flux might be faint depending on the star distance, but the required information is even harder to access. Actually, the investigated information is contained in the spectrum shape of this weak incoming light. Hence in the case of exoplanet investigation, what matters above all is once more the detection performances in terms of QE and dark noise i.e. dark current.

Moreover, the exoplanet is usually not directly imaged by the system so that the focal plane array format and pitch are not critical in this latter case, as opposed to more usual astronomy imaging observations. In this case, the observed objects are usually under-sampled by the focal plane array (regarding optics F# and/or atmosphere turbulences) and the system do not push for small pixels. In contrast, what matters above all for more conventional astronomy imaging is not only the array format but also the overall detection surface in order to perform radiometric estimations on a large scale. Indeed, astronomy usually requires very large focal plane arrays (typically several megapixels) with relatively large pixels pitches (typically larger than 15µm). The case of hyperspectral imaging is even more stringent. In such systems, the incoming light is usually spread depending on its wavelength with a prism or a grating. The detection array is then used to sense the resulting light: each pixel receives a different wavelength than its neighbor. In that case, the array format, at least in one given direction, represents the spectrum resolution and has to be as large as possible. Moreover, the flux sensed by the pixels is very low (due to the spectrum dispersion) and therefore the pixel size has to stay relatively large to be able to integrate this low flux conveniently.

Of course, low flux detection calls for low dark currents. A high performance photodiode is usually limited by diffusion currents at high temperatures whereas it might be limited by depletion currents at lower temperatures [1]. Diffusion currents I_{diff} evolve proportionally to the square of intrinsic carrier concentration n_i of the semiconductor material where diffusion occurs, which gives in the 1D case:

$$I_{diff} = q \frac{n_i^2}{N_d \times \tau} th_{diff} A_{px} \propto \exp\left(-\frac{E_g}{kT}\right) \tag{1}$$

With q the charge of the electron, N_d the doping concentration of the diffusion layer, τ the minority carrier lifetime, th_{diff} the diffusion layer thickness, A_{px} the pixel area and k and T the Boltzmann constant and absolute temperature respectively.

On the other hand, depletion currents are dark currents originated in the junction space charge region and are proportional to the intrinsic carrier concentration of the semiconductor where this depletion region extends giving:

$$I_{dep} = q \frac{n_i}{2\tau_{SRH}} W_{dep} A_{dep} \propto \exp\left(-\frac{E_g}{2kT}\right) \tag{2}$$

Where τ_{SRH} stands for the Shockley-Read-Hall lifetime in the depletion volume, W_{dep} and A_{dep} for the thickness and area of this depletion region . Note that through τ_{SRH}, this depletion current is also proportional to the density of material defects (giving mid-gap recombination traps), which therefore strongly depends on semiconductor crystal quality.

Consequently, what defines the corner temperature between those two regimes is the ratio between the gap E_g of the semiconductor sensitive material and the thermal energy expressed by kT. A high E_g/kT ratio defines detection conditions where diffusion current tends to be easily dominated by depletion current.

In this context of science detection, do NIR and LWIR low flux detections require different approaches? First of all, the specifications are very different. 0.1^e/s are usually required for NIR observations for astrophysics, at 100K typical operating temperatures. For a 2µm cut-off, this leads ratios close to $E_g/kT \sim 75$, closer to 60 for 2.5µm cut-off. On the other hand, LWIR specifications for exoplanet detection requirement is typically 500^e/s at 12.5µm - 40K, for a typical ratio half this value: $E_g/kT \sim 30$. Hence, given the typical operating temperature, NIR conditions are usually twice sensitive to depletion currents than LWIR conditions. In this case, a very close attention to the space charge region volume extension in the narrow gap must be taken during the photodiode design in order to minimize depletion current. Moreover, the level of dark current is so low that even very small shunt currents (through passivation or under-filling) might become limiting factors. On the other side, LWIR focal plane arrays must remain diffusion limited at 40K to meet the required specifications. This means that depletion currents but also tunnel currents has to be both minimized. Tunnel currents are very specific to very narrow gap photodiodes as it is the case in the LWIR range. Their mitigation usually require low doping and smooth doping profile junctions [2 3].

In the end, the common denominator between all those low flux detectors is the depletion current mitigation. This requires a very high quality semiconductor material to avoid recombination centers which are sources of depletion currents. To reach such level of performances, every step of the fabrication process must be carefully optimized, from the CdZnTe substrate, the active layer CdHgTe growth, the passivation and all the fabrication processes [4].

III. NIR ARRAYS FOR ASTROPHYSICS

During the last five years, a strong effort has been carried out at CEA-LETI (French atomic energy commission, Electronic division), CEA-Sap (French atomic energy commission, Astrophysics service) and Sofradir, in order to investigate the feasibility of NIR focal plane arrays for astronomy. Such arrays are already available from one single US Company [5]. However, for political issues, European astronomers are willing for a second source, free of political issues (the delivery of such arrays is considered as war material and subject to very stringent exportation rules). Hence, the framework of this activity was an ESA (European Space Agency) contract aiming at building a European source for focal plane array suitable for astrophysics needs. Figure 1 sums up data obtained in terms of dark current with extrinsic p/n diodes (down oriented triangles) and intrinsic n/p diodes (up oriented triangles). Both MBE and LPE growth methods are compared. The plot also compares those results with other programs using avalanche photodiodes (APD, clear blue symbols and curves) made for another program. Those various datasets have been measured with different read out input circuits (ROIC). The first two were based on a source follower per detector (SFD) input stage well suited for very low flux values [6]. The last one was a capacitive trans-impedance amplifier per pixel (CTIA), dedicated for ultra-fast measurement (RAPID ROIC, [7]), less suited for very low fluxes.
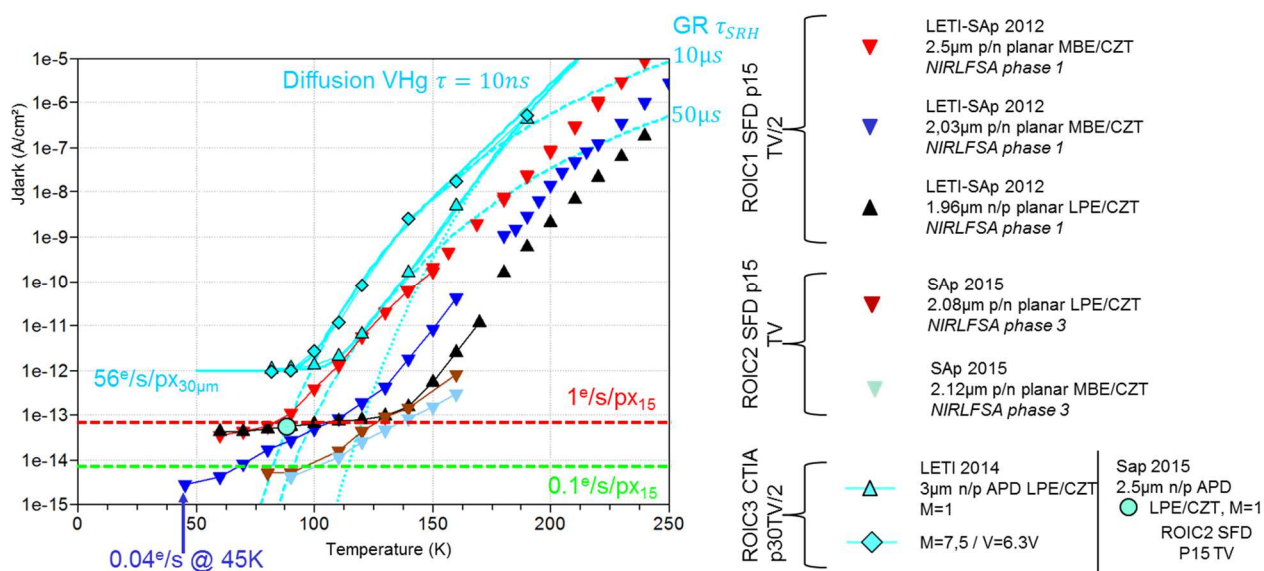

Figure 1 : Dark current data for NIR p/n and n/p arrays (2.08 and 2.12µm data is corrected from ROIC glow)

As a reminder, intrinsic n/p diode are the legacy technology used at LETI-Sofradir. Due to the fact that p type doping is done using intrinsic Hg vacancies (VHg), the minority carrier lifetime of the diffusion layer is low, degrading the diode performances. Extrinsic p/n diodes are a newer diode technology transferred from LETI to Sofradir. In that case, the diode structure is inverted and doping is obtained with incorporation of extrinsic doping elements (Indium during growth for the N type diffusion layer, and Arsenic ionic implantation for the P type collecting part) and the minority carrier lifetime is supposed to be much higher, leading to an important gain in terms of dark current. Due to the planar structure used and the high absorption coefficient of CdHgTe, the obtained quantum efficiencies (QE) are usually very high (70% and above), as shown on Figure 2.

In Figure 1, n/p data is represented by black down triangles and stands for one processed layer cutting at 1.96µm (all NIR cutoffs are given at 78K in this part). Data follows the expected diffusion trend line at high temperatures: the dark current strongly decreases cooling down the detector. Below 150K, this dark current reduction saturates, down to values close to 1e/s. P/n data reported in Figure 1 addresses different wavelengths: red symbols stand for 2.5µm cutoff diodes, whereas other colors (deep blue, lighter blue and brown) stand for shorter cutoffs (respectively 2.03, 2.12 and 2.08µm). MBE p/n diodes 2.5µm cutoff and LPE n/p diodes 1.96-µm cutoff exhibit a common low temperature current plateau at 1e/s. This suggests a common limitation independent on material growth method, cadmium composition and diode structure. However, a third layer cutting at 2.03µm shows much lower dark currents with p/n diodes, down to 0.04e/s at 45K, suggesting that the characterization bench is free of photonic leakage.
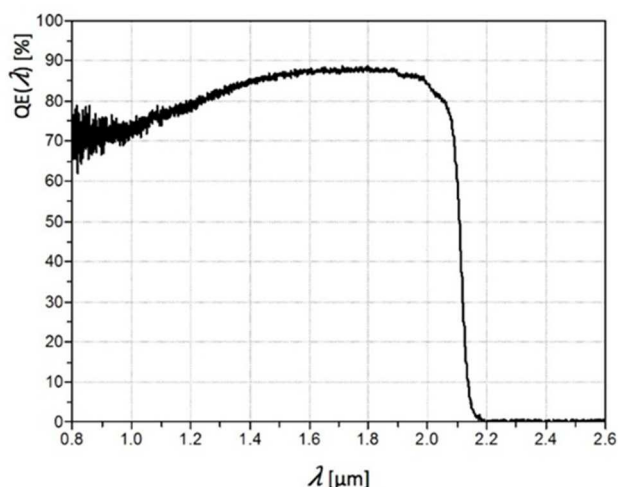
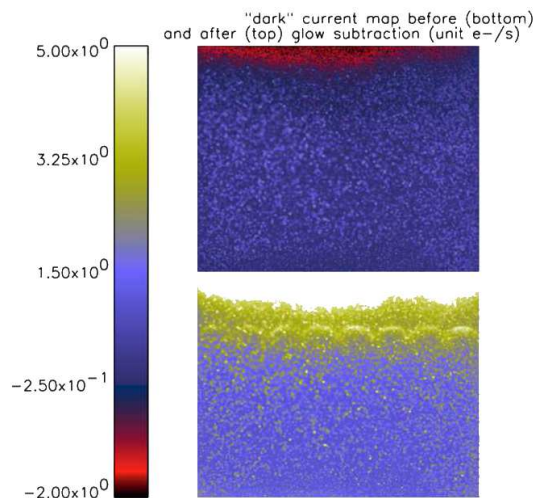**Figure 2 : Typical spectral QE measured at 80K on NIR diodes discussed**

Figure 3: Image of a NIR detector at dark at 100K before and after subtraction of glow current

Note also that the first two layers (2.5 and 2.03µm cutoffs) were processed with a higher doping than the other layers, so that dark current at high temperatures (in the diffusion regime) is not optimal. On the other hand, the last two layers (cutting at 2.08 and 2.12µm) where lower doped. Note as well that two different growth processes have been used for those last two layers: MBE and LPE. Measurements showed no major difference in the dark or photonic current mappings: the two arrays performances were very close at 100K. Deeper analysis of the results and characterization of those two last layers are presented in a dedicated paper [8]. Very low dark current values were limited by Si glow below 1e/s, either from the ROIC or from the temperature probes used in the characterization bench. Moreover, n/p data (black up triangles) and 2.5µm p/n (red down triangles) seem limited by the same mechanisms, probably ROIC glow as well. However, when free of ROIC glow as is the case of 2.03µm p/n data (blue down triangles), the estimated dark current can be very low, below 0.1e/s for a 15µm pitch pixel, compatible with astronomy observation specifications. During the last phase of the project, evidence of ROIC glow from the eight output amplifiers are clearly seen on current mapping measured at darkness (Figure 3). A numerical subtraction allows us an estimation of the intrinsic limitation of the photodiodes once again below 0.1 e/s at 100K compatible with the required specifications (light blue and brown down triangles in Figure 1, see [8] for further details). The next phase of this activity will be to demonstrate the fabrication of larger arrays. Sofradir has already demonstrated the ability to hybridize 1kx1k array at 15µm with the highest level of performances [9], but even larger arrays (2kx2k at least) have to be demonstrated to catch up with the existing Hawai arrays actually used by the astronomers [10].

HgCdTe avalanche photodiodes (APD) are particularly suitable for low flux detection. Indeed, the possibility to pre-amplify the incoming photonic signal into the photodiode itself (with no major degradation of the signal to noise ratio [11]) is very interesting when the detection performance is limited by the ROIC noise as it is the case in the very low flux detection for astronomy. The APD data reported in Figure 1 has been measured on a 30µm pitch 320x526 focal plane array with 3µm cutoff. Without gain (low applied bias, clear blue up triangles), the measured data is consistent with 10ns lifetime for the diffusion regime at high temperature (typical value expected given the VHg doping used). At intermediate temperature (between 110 and 140K) the measured data is consistent with a depletion current with 50µs SRH lifetime. At even lower temperatures, the measured dark current saturates at 56e/s/pixel. With a 6.3V applied bias, the mean APD gain is $M = 7.5$. Normalized by this gain, the dark current measured under this bias condition is given by the diamond clear blue symbols. This latter data is again consistent with 10ns diffusion lifetime and 10µs depletion SRH lifetime (taking a larger space charge region due to the depletion extension under large bias). Again, the input current decrease saturates at 56e/s/pixel at temperatures below 100K. Unfortunately the ROIC input stage used for this APD array was not designed for low flux detection and seemed limited by a strong ROIC glow at low temperatures. As a matter of consequence, it was not possible to estimate the real dark current behavior of our APDs at low temperatures. It is however possible to extrapolate depletion at lower temperatures given the extracted lifetimes at intermediate temperature (depletion trend line). In that case, the dark current should be close to the typical specifications for astronomy systems, given the fact that the cutoff of those APDs is much larger (3µm) than the requested cutoff for astronomy (2.5µm).

Very recently, LETI has fabricated APD arrays with the targeted 2.5µm cutoff, compatible with the SFD ROIC used for the preceding p/n arrays that should give access to very low dark currents at low temperatures. Unfortunately, the SFD input stage didn't allowed us to operate at the high voltages required for the APD gains. However, measurement carried out at low biases (unity gain) at 80K showed 0.9e/s dark currents, consistent with previous extrapolated values. In terms of additional noise due to the impact ionization process, high flux characterizations showed that typical excess noise factors exhibited peak histograms below 1.2 [12]. This early stage experiment tends to demonstrate that APD array might be well suited for low flux detection in the NIR range, at the expense of a slightly higher operating temperature to counterbalance a slightly higher dark current under high biases.

IV. MWIR-LWIR FOR EXOPLANET INVESTIGATION

The next part of the paper deals with results obtained for longer wavelengths arrays for science purposes, mainly for exoplanet observation. Again the framework of this activity was ESA and CNES contracts to investigate the feasibility of such systems. Three channels were investigated with LPE grown material: MWIR channel with n/p VHg diodes (5.5µm cutoff at 78K), LWIR- with 9.5µm cutoffs at 78K also with n/p VHg diodes, and longer diodes (LWIR+, 12.5µm cutoff at 40K) with p/n extrinsic diodes. All arrays were hybridized onto a study ROIC, 320x256 format 30µm pitch with a 500fF integration capacitance. The input stage of this ROIC was a CTIA, compatible with both polarities and allowing nondestructive readings to be able to use the follow up the ramp (FUR) integration scheme with integration times as large as several minutes. The first characterization step was the evaluation of the ROIC for very low current level, of the order of only several hundreds of e/s. Thanks to this FUR mode, leakage current as low as 2 e/s has been observed onto a bare ROIC for a temperature range between 16 and 120K.

For every channel, different diode geometry were available. The idea was to investigate different space charge region volume to work on depletion current. Those different diode variations lead as expected to different low temperature currents but also to different QE (related to different pixel fill factors). Fortunately several variations appeared optimal in terms of QE. An example of MWIR channel spectral QE is given in Figure 4 showing that QE higher than 60 to 70% are obtained, whatever the temperature between 20 and 78K. The corresponding dark current is given in Figure 5.
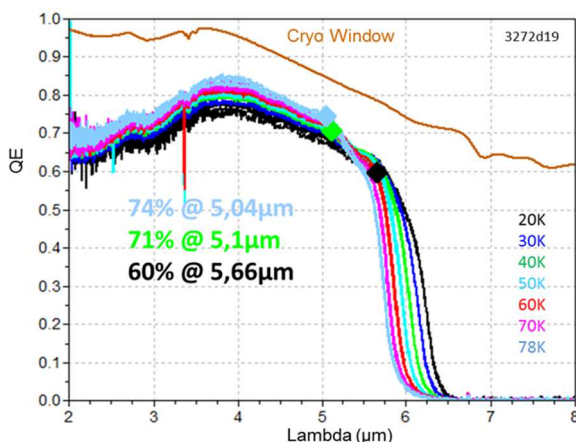

Figure 4 : Typical spectral QE measured on MWIR channel diodes
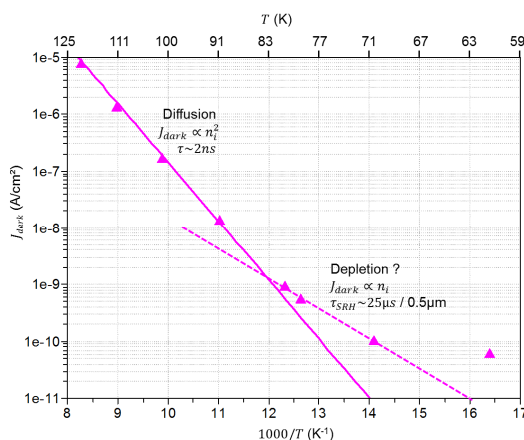

Figure 5 : Focus on MWIR data from Figure 6

Measured diffusion currents appear consistent with 2ns lifetime for temperatures above 90K, as expected from VHg diodes. Below this temperature, this dark current saturates close to a couple of thousand e/s. The meaning of this low temperature leakage regime is still to be clarified, as the same level of leakage current has also been observed on other FPAs corresponding to other cutoffs (see Figure 6). Between diffusion and saturation, some data points may be seen consistent with depletion current with 25ns SRH lifetime. However, this potential depletion regime is given on a limited temperature range, containing only three data points and remains therefore highly doubtful.

For more clarity, Figure 6 gathers the three channels dark current data corresponding to high QE diode variations. At high temperature (above 50K), LWIR- data (blue up triangles) is again consistent with expected diffusion lifetime limited by VHg. Dark current saturation occurs at the same level of current as MWIR data (purple up

triangle), but at a much lower temperature. Between 50 and 25K, an intermediate regime is observed, where the activation energy is not consistent with half the gap of the absorbing material as expected from depletion current. Surprisingly, in this regime, the activation energy is closer to a fourth of the gap than half the gap (as would be expected from a classical depletion current limitation).

Concerning extrinsic p/n LWIR data (red down triangle in Figure 6), the diffusion dark current is very similar to LWIR- intrinsic data despite the cutoff difference, because of the gain in lifetime (from ns to μs) switching from intrinsic to extrinsic doping. In addition, p/n measured diffusion current is consistent with rule07 [13] as usually observed with LETI-Sofradir p/n diodes. However, low temperature leakage currents appear lower for p/n data than n/p data, dismissing a potential limitation due ROIC leakage or glow. Once more, low temperature decrease is not consistent with classical depletion activation energy at half the gap. Between 40 and 20K, the observed activation energy is again closer to a fourth of the gap rather than half the gap, decreasing down to very low dark current values (below 100e/s).
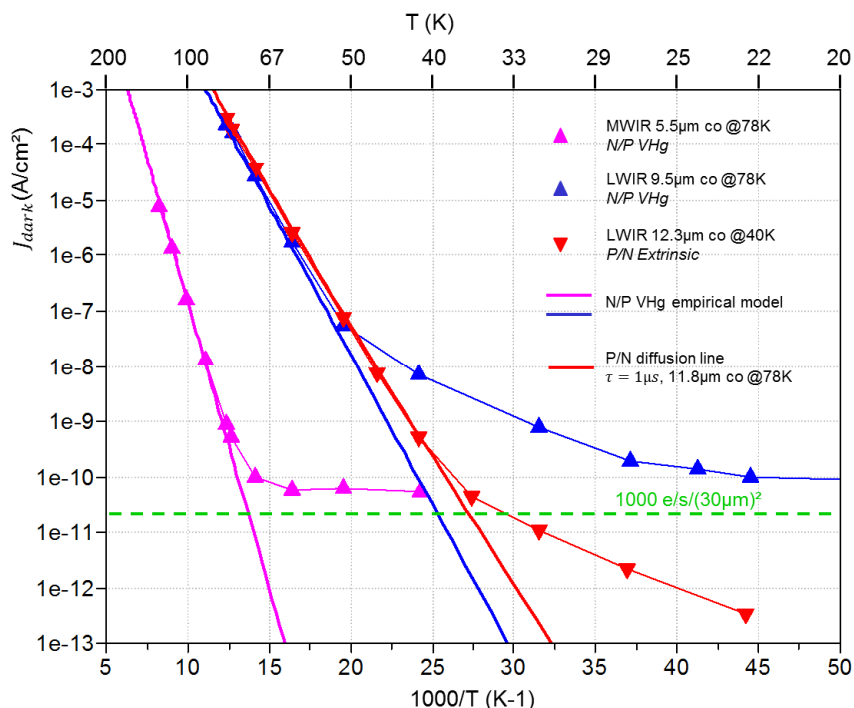

Figure 6 : Arrhenius plot with dark current data for MWIR-LWIR n/p and p/n data

In terms of photonic current, p/n LW+ diodes behave differently than n/p VHg diodes. Despite the increasing gap with decreasing temperature, p/n diodes exhibit a strongly decreasing photonic current at low temperatures (below 50K). This effect is also seen on spectral QEs measured at different temperatures (80 to 20K) as shown on Figure 7. As can be seen on the plot, the cutoff wavelength increases with decreasing temperature consistently with Hansen's law [14]. Except for a response dip at 8μm (due to known imperfections of the mirror coating of the test bench) and below 3μm where the test bench is not optimize, the rest of the spectral QE remains quit flat at all temperatures. However, the absolute level of QE decreases from 70% at 70K and higher to 20% at 20K. Further study based on variable diameter test single diodes showed that this QE decrease might be due to diffusion length contraction with temperature. Indeed, the photonic current measured on those variable area diodes allows the estimation of this lateral diffusion length. Using a given a given set of geometries (diodes with diameter ranging between 120μm to 10μm), the general principle is to search a lateral collection length consistent with a photonic current density independent on the diode diameter. This method is in fact an efficient way to estimate this diffusion length Ld at different temperatures [15]. Figure 8 shows the evolution of the estimated Ld as function of the temperature. Diffusion length values range from 16μm at 80K to 6μm at 20K. With decreasing temperature the diffusion length starts to strongly decrease around 60K-50K. Due to Ld values reported Figure 8 and diode geometries used in the tested arrays, we can conclude that the optical Fill Factor (FF) becomes lower than unity for temperature lower than 50K, thus explaining the observed QE loss in Figure 7. One way to compensate this is to reduce the FPA pitch while keeping the same implanted surface in the diode. A 15μm pitch (instead of 30μm) should be efficient to obtain a FF close to unity at low temperature and thus recover a high QE.
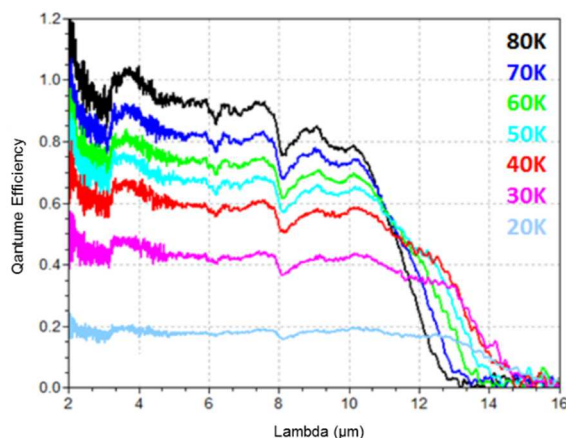
Figure 7 : Spectric quantum efficiency measured on p/n LW photodiodes for temperatures ranging for 80 to 20K
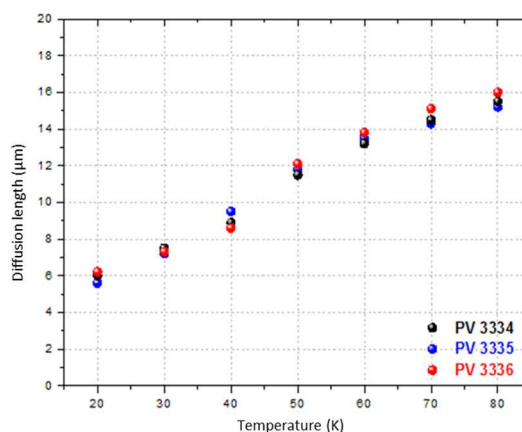

Figure 8 : Lateral contribution of the optical area estimated from different radius p/n LW photodiodes

V. VLWIR FOR ATMOSPHERIC SOUNDING

The last part of this paper deals with VLWIR FPA for atmospheric sounding. In this case, the aim is a spectroscopic analysis of the atmosphere using the earth as a black body source. Usually, several bands are concerned, from SWIR to LWIR. In that system, the VLWIR band (14.5µm) is very important for atmospheric sounding because it corresponds to a very specific CO_2 absorption peak, allowing the estimation of the temperature profile of the sounded atmosphere layers. However, this band is very challenging because it corresponds the lowest energy photons. The development of such VLWIR focal plane arrays based on LPE HgCdTe first started in 2005 at LETI-Sofradir under CNES contract in order to prepare Meteosat Third Gen (MTG) pre-design phase. The evaluated structure was based on n/p diodes and ended up to fully functional 320x256 arrays with cutoffs close to 19µm at 50K [16]. This activity was followed by an ESA contract to target more specifically the 14.5µm cutoff required by the MTG needs [3], using the classical n/p diode configuration. Arrays showed very good performances in terms of QE, noise and defectivity. All dark currents obtained with VLWIR diodes followed the expected diffusion trend line at 78K as can be seen in Figure 9 (blue square symbols). This diffusion behavior was observed down to relatively low temperatures (down to 30K for a cutoff close to 20µm). This activity ended up with the selection of Sofradir as the sole supplier of IR focal plane arrays for the MTG program. In parallel the evaluation of p/n extrinsic diodes in this wavelength range came rapidly as an evidence, in order to lower the dark current ie increase the operating temperature. Throughout the years, different LPE metallurgical points were evaluated to investigate the potentiality of this technology in VLWIR. This process being relatively young (as opposed to the legacy n/pVHg process), the learning curve took longer in order to obtain uniform arrays. In particular, the p/n diode being an abrupt diode (as opposed to n/p diodes witch include an N- intrinsic region between the N+ collecting contact and the P type diffusion layer), special care was necessary for the management of tunnel currents.

In terms of dark current, the different values obtained at 78K are gathered onto Figure 9 (black diamond). Data perfectly follows the diffusion line represented by rule07 in dotted lines [13]. Very recently in 2015, several points have been added to this curve (represented by four colored diamond symbols in Figure 9) for extremely long cutoff wavelength (between 15.5µm and up to 17.3µm at 78K). The mid response cutoffs measured on such diodes perfectly follows the expected Hansen's law [14] down to 50K, giving values ranging from 17.5µm up to 19.7µm at 50K, with a classical wideband uniform spectral QE, from MWIR to LWIR and VLWIR [17], corresponding to cadmium composition below 0.2 (0.1957 to 01917).

An example of I(V) characteristics measured on such VLWIR diodes at darkness is given in Figure 10. As can be seen, tunnel currents are quite strong for high biases, limiting the extension of the polarization plateau. However, when polarized to low biases, below 100mV, fully functional array were obtained with those layers. In those conditions, the measured current follows a diffusion trend line down to 50K, with an activation energy corresponding to the gap estimated from the measured cutoffs. Note moreover that such a behavior deviates from rule07. Indeed, as we previously mentioned [18] in the case of LWIR-VLWIR diodes cooled down below 80-50K, measured dark current is always higher than rule07 whatever the technology or the growth process so that rule07 might not be used to estimate dark current in this temperature range. This has been also observed on data from other HgCdTe FPA suppliers.
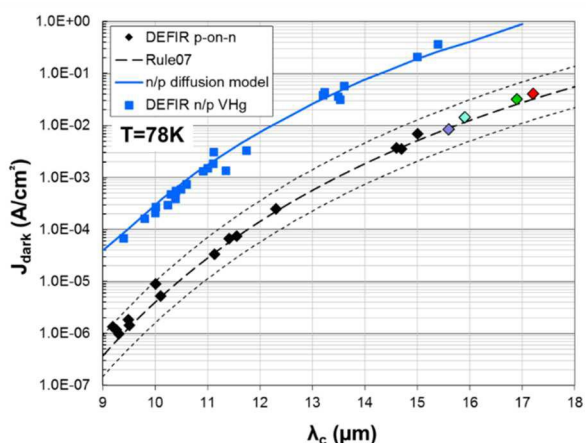
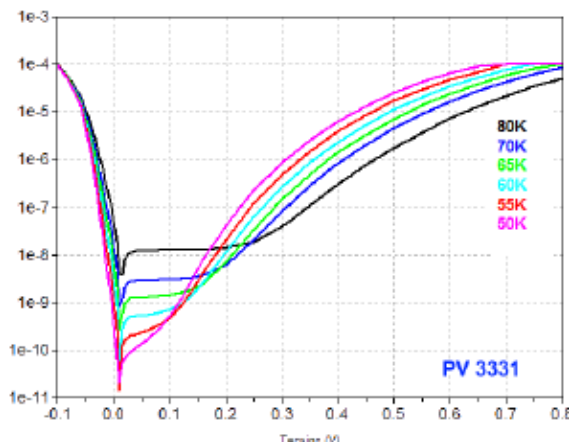**Figure 9 : Summary of dark currents measured at 78K for both n/p and p/n diodes from LWIR up to VLWIR spectral ranges**

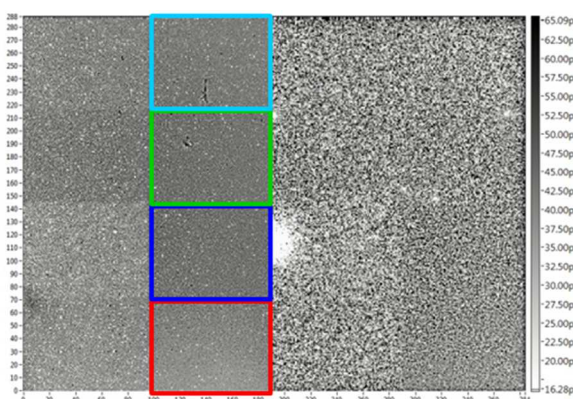**Figure 10 : Typical I(V) measured on 30µm pitch VLWIR p/n diodes**

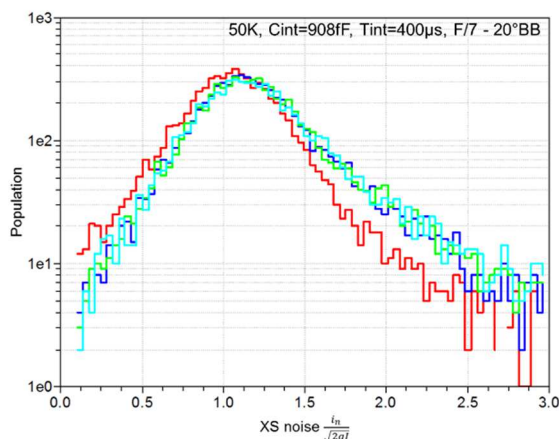**Figure 11 : Current mapping obtained on a 320x256 30µm pitch p/n VLWIR array at 50K (grey scale in A)**

Figure 12 : Excess noise statistics obtained on FPA variant of Figure 11

320x256 arrays with 30µm pitch were hybridized onto a direct injection (DI) ROIC. Those FPAs being study arrays, several diode variations where designed onto the same array to fasten up characterization and analysis (16 variants per FPA, giving a total of 5100 diodes per variant). Studied parameters were mainly diode geometries and interpixel passivation. Figure 11 gives a current mapping obtained on such array at 50K with a 408fF integration time, 400ns integration time and F/7 ambient illumination. Obviously, some diode variations exhibit bad uniformity and current leakage, as can be seen on variant on the right hand side of the mapping. However, some diode variations are fully functional. These variants show very good uniformity, highlighted in color in Figure 11. Last but not least, these diodes exhibit very good noise features. Figure 12 shows excess noise distributions measured on these four variants. Excess noise is defined as the ratio between measured rms noise i_n and expected shot noise $\sqrt{2qI}$ given the measured current I. This excess noise ratio is computed for each pixel and the resulting histograms are plotted for each different variants (four colors in Figure 12). Gaussian shapes are obtained, with a peak value close to unity (between 1 and 1.1) and typical standard deviations between 10 and 11%. Those noise distributions might even be plotted in log scale showing very low distribution tails, i.e. very high operabilities, higher than 99.8% with classical criterions (30% on responsivity and 50% on noise). To our knowledge, those FPAs are the longest HgCdTe arrays ever processed.

VI. CONCLUSION

HgCdTe for space and science imaging is very demanding in terms of detection performances: high QE and low dark currents are mandatory. Strong effort has been carried out during the last few years at LETI and Sofradir for such applications. p/n NIR diodes now exhibit features compatible with low flux astronomy needs, both for LPE and MBE grown material [19] and effort should now focus on larger format arrays. However, n/p APDs could also be a viable solution, with a potential gain in ultimate performances thanks to noiseless gain. Longer wavelength has also been actively investigated for exoplanet study. n/p VHg doped MWIR and LWIR diodes have been deeply characterized down to very low temperatures, followed also by p/n LW diodes. High QEs and dark currents lower than 1000e/s has been already demonstrated and optimization of such diodes for ultra low fluxes is still under active investigation for the LWIR range. Last but not least, VLWIR p/n focal plane arrays have been also studied for atmospheric sounding. Full performance functional arrays have been successfully demonstrated with cut-offs ranging between 15.5 and 17.5µm at 78K, corresponding to 17.5 to 19.7µm at 50µm.

VII. ACKNOWLEDGMENTS

VII. REFERENCES

[1] Gravrand, O., Mollard, L., Boulade, O., Moreau, V., Sanson, E., & Destefanis, G., *JEM.*, *41*(10), 2686, (2012).

[2] Gravrand, O., Borniol, E., Bisotto, S., Mollard, L., & Destefanis, G, *JEM.*, *36*(8), 981, (2007).

[3] Gravrand, O., Mollard, L., Largeron, C., Baier, N., DeBorniol, E., & Chorier, P., *JEM*, *38*(8), 1733, (2009)

[4] Gravrand, O., Destefanis, G., Bisotto, S., Baier, N., Rothman, J., Mollard, L., *JEM*, *42*(11), 3349 (2013)

[5] Beletic J. ; Blank R. ; Gulbransen D. ; Lee D.; Loose M. ; Piquette E. ; Sprafke T. ; Tennant W.; Zandian M. ; Zino J., Proc. SPIE 70210H; (2008)

[6] Fièque, B., Martineau, L., Sanson, E., Chorier, P., Boulade, O., Moreau, V., & Geoffray, H., Proc. *SPIE*, *8176*, 81761I–81761I–13, (2011)

[7] Guieu, S., Feautrier, P., Zins, G., Le Bouquin, J.-B., Stadler, E., Kern, P., Bourget, P., Proc *SPIE*, 91461N, (2014)

[8] Cervera, C., Gravrand O., Zanatta J.P., Lobre C., Santailler J.L., Boulade O., Moreau, V., , *JEM* (2016)

[9] Delannoy A., Fièque B., Chorier P., Riuné C, SPIE 96390R, (2015)

[10] J.W. Beletic et al., Proc. SPIE 7021, (2008)

[11] Perrais, G., Gravrand, O., Baylet, J., Destefanis, G., & Rothman, J. , *JEM.*, *36*(8), 963, (2007)

[12] De Borniol, E., Rothman, J., Salveti, F., & Feautrier, P., *ICSO2014* p. 65468. Tenerife. (2014)

[13] Tennant, W. E., Lee, D., Zandian, M., Piquette, E., & Carmody, M., *JEM.*, *37*(9), 1406, (2008)

[14] Hansen, G. L., Schmit, J. L., & Casselman, T. N., *J. Appl. Phys.*, *53*(10), 7099, (1982)

[15] Cervera, C., Baier, N., Gravrand, O., Mollard, L., Lobre, C., Destefanis, G., Moreau, V., Proc. *SPIE*, 945129, (2015)

[16] Gravrand, O., Borniol, E., Bisotto, S., Mollard, L., & Destefanis, G., *JEM*, *36*(8), 981, (2007).

[17] Cervera, C., Baier, N., Gravrand, O., Mollard, L., Lobre, C., Destefanis, G., … Moreau, V., Proc. *SPIE*, 945129. (2015)

[18] Baier, N., Cervera, C., Gravrand, O., Mollard, L., Lobre, C., Destefanis, G., Moreau, V., *JEM.*, *44*(9), 3144, (2015).

[19] Crouzet P.-E.; Duvet L.; de Wit F.; Beaufort T.; Blommaert S.; Butler B.; Van Duinkerken G.; ter Haar J.; Heijnen J.; van der Luijt K.; Smit. H., SPIE 96390X; (2015)